हर कदम, हर डगर
किसानों का हमसफर
भारतीय कृषि अनुसंधान परिषद

Agrisearch with a human touch

All India Coordinated Research Project on Agrometeorology
ICAR-Central Research Institute for Dryland Agriculture
Santoshnagar, Hyderabad-500 059

Network of Automatic Weather Stations:
An AICRPAM-NICRA Initiative

All India Coordinated Research Project on Agrometeorology
ICAR-Central Research Institute for Dryland Agriculture
Santoshnagar, Hyderabad-500 059

Network of Automatic Weather Stations:
An AICRPAM-NICRA Initiative

P. Vijaya Kumar, A.V.M. Subba Rao, Sarath Chandran M.A., Sandeep V.M., Pramod V.P., Rajkumar Dhakar, S.K. Bal, V.U.M. Rao and K. Sammi Reddy

All India Coordinated Research Project on Agrometeorology
ICAR- Central Research Institute for Dryland Agriculture
Santoshnagar, Hyderabad - 500059

Citation:
Vijaya Kumar, P., Subba Rao, A.V.M., Sarath Chandran M.A., Sandeep V.M., Pramod V.P., Dhakar, R., Bal, S.K., Rao, V.U.M. and Sammi Reddy, K. 2018. Network of Automatic Weather Stations: An AICRPAM-NICRA Initiative. ICAR – Central Research Institute for Dryland Agriculture, Hyderabad – 500059, 40 pp.

Copies: 200

Published by
Director
ICAR-Central Research Institute for Dryland Agriculture
Santoshnagar, Hyderabad - 500059
Ph: 91-040-24530177, 24530161 (O)
Fax: 91-040-24531802
Web: http://www.crida.in
E-mail: director.crida@icar.gov.in

Technical Assistance: I.R. Khandgonda

Cover page design: A. Mallesh Yadav

Printed at:
Balaji Scan Private Limited,
Flat No. 202, Opp. Krishna Children Hospital,
Lakdikapul, Hyderabad-500004.
Tel: 23303424/25, 9848032644

Contents

1. Introduction

Agriculture that forms the backbone of Indian economy is dependent on weather and climate. Therefore, the change in climate has become an important area of concern for India to ensure food and nutritional security for a growing population. The climate change and variability are already visible in observed temperature and rainfall. For instance, the air temperature on global and regional scale increased in the 20th century with the largest warming occurred in the last 30 years (WMO, 2005). The year 2014 was found to be the warmest year in the entire record for which measurements are available. The difference between maximum and minimum temperature is narrowing, which could be detrimental for agriculture (Easterling et al., 1997, Bapuji Rao et al., 2015). Significant changes have also been noticed in climate variables (i.e. precipitation and air temperature) across India during the period of 1950-2008 (Mishra et al., 2014a, 2014b). Declining trends in the observed precipitation during the monsoon season were noticed (Mishra et al., 2012), which were partially associated with the warming in the Indian Ocean (Alory et al., 2007; Brown and Funk, 2008). An increase in mean air temperature was reported globally (Karl et al., 1996). At the regional scale, precipitation declined while temperature increased over the major area of India in the last few decades, which caused increased frequency of droughts and reduction in soil moisture for crop growth (Mishra et al. 2014).

The increase in air temperature and decreases in rainfall could lead to persistent moisture deficit conditions that can hamper the crop production in India. Under the current and projected future climate, the frequent droughts during the monsoon season can cause enormous challenges for crop production in India (Mishra et al., 2014). The likelihood of drought occurrences might further enhance in future with significant increase in temperature and heat waves, number of hot days and hot nights as well as decrease in precipitation. The impacts of drought and climate variability and changes on agricultural production are well documented (Lobell and Asner, 2003; Lobell and Field, 2007; Mishra and Cherkauer, 2010; Mishra et al., 2014). Modelling studies show that for every 1 °C increase in seasonal temperature, the grain yield might decline by 2.5% to 16%

in the sub-tropics and tropics (Lobell et al., 2008; Battisti and Naylor, 2009). The gap between crop production and consumption will increase especially in the developing countries in changing climate (Fischer et al., 2005) and the impacts of climate change on food security could be even more, than previously thought (Schmidhuber and Tubiello, 2007).

2. Need for Automatic Weather Station

The observations of surface meteorological parameters are important in understanding the spatio-temporal variations in weather and climate. The conventional, manned, surface observatories established by India Meteorological Department (IMD) at a resolution of 100-200 km is not adequate to meteorologically represent regions having diverse seasonal weather patterns. Moreover, the surface meteorological observatories are established only at places, which are well connected in terms of transport and telecommunication network. Need has been felt since long to have continuous weather monitoring over the Indian sub-continent, particularly of remote/ inaccessible places including river catchment areas and snow bound mountains. Data from coastal/remote areas during adverse weather conditions like that of a cyclonic storm or passage of western disturbances are crucial for weather forecasting. With this idea, automation by installation of Automatic Weather Stations (AWS) was envisaged so that human intervention can be minimized.

According to the World Meteorological Organization (WMO), an automatic weather station (AWS) is defined as a "meteorological station at which observations are recorded and transmitted automatically" (WMO, 1992a). Automatic weather observation refers to the activities involved in converting measurements of meteorological elements into electrical signals through sensors, processing and transforming these signals into meteorological data, and transmitting the resulting information by wire or radio or automatically storing it on a recording medium. AWSs can be divided into two categories such as Real-time AWSs and Offline AWSs.

Real-time AWS: It is a station that records observations on a real-time basis, either regularly or upon request by the user. This type of station is used for ordinary synoptic meteorological analysis and monitoring of storms and river or tide levels. It must be able to transmit observations to a network.

Off-line AWS: A station that records observations on storage devices. This type of station is used for climatological analysis or as an auxiliary facility to manual observations. The data obtained and stored by an off-line AWS need to be transmitted to the user at regular intervals.

The following advantages can be expected from automatic weather stations:

- Continuous observation is possible, and data at AWS stations can be obtained even when no staff is present. Fully automated systems can also be installed at inaccessible sites. In addition, it is possible to reduce number of observations and operating costs.
- Since meteorological data are taken as electrical signals, errors while taking observations are eliminated. Standardized observation techniques enable the homogenization of observed data in regions where automatic weather observation is adopted. In addition, new observation elements can be added relatively easily by installing new instruments.
- Optimal measuring instruments with the appropriate level of measurement accuracy for the required observation can be chosen, and there is no need for training the observers.

3. AWS Network under NICRA Project

National Innovations in Climate Resilient Agriculture (NICRA) is a network project (http://nicra-icar.in/nicrarevised/index.php/en/home) of the Indian Council of Agricultural Research (ICAR) launched in February, 2011. The project aims to enhance resilience of Indian agriculture to climate change and climate vulnerability through strategic research and technology demonstration. The research on adaptation and mitigation covers crops, livestock, fisheries and natural resource management. The NICRA project has three components

a. Strategic research on adaption and mitigation on important grain and horticulture crops critical for food security, livestock and fisheries.

b. Technology demonstration in 100 most vulnerable districts on best bet practices to cope with current climate variability.

c. Capacity building of different stakeholders (scientists, policy makers, extension staff and farmers) on climate change.

Among the three components, demonstration of the existing technologies to cope with current climate variability are being undertaken in 100 districts (**Annexure-I**) through KVKs and climatic variability is being assessed by All India Coordinated Research Project on Agrometeorology (AICRPAM) through collecting and analyzing climatic data. Thus, AICRPAM is entrusted with acquainting and maintenance of quality data by installing Automatic Weather Stations (AWS) in each district under the NICRA scheme. The 100 locations as representing various climatic vulnerabilities were identified and presented in **Fig.1**.

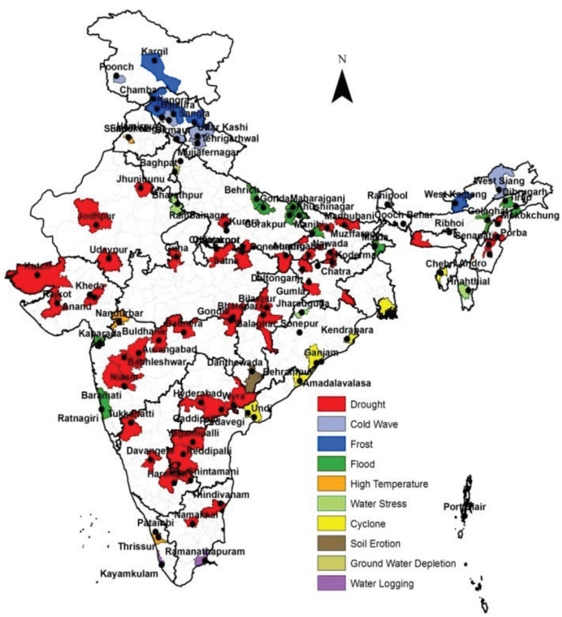

Fig.1: NICRA-AWS locations based on climatic vulnerability

4. Technical Specification of NICRA-AWS

The NICRA AWS is recording 7 meteorological parameters such as temperature (maximum & minimum), relative humidity (maximum & minimum), wind speed, wind direction, solar radiation, rainfall and evapotranspiration. Out of these, evapotranspiration is a derived parameter calculated using FAO Penman Monteith Method. The NICRA-AWS uses high quality sensors in recording these meteorological parameters. Several factors were considered in selecting the sensors for use in AWS network. The foremost important factor is the compatible of the sensors with the AWS data logger. Accuracy, resolution and response time were the other factors considered for selection of sensors. The technical specifications of each meteorological sensor and a layout picture of AWS are shown in **Table 1** and **Fig.2**, respectively.

Table 1: Technical specification of sensors used in NICRA-AWS

Parameter	Sensor	Specifications
Temperature & Relative Humidity	Rotronic's AT/RH Sensor (HC2-S3)	Temperature Range: -50 to 100 °C Accuracy: ± 0.5% @ -10 to 70 °C Resolution: 0.02% Typical RH Range: 0 – 100% Accuracy: ± 0.8%
Wind Speed & Direction	RM Young 85000 Ultrasonic Anemometer	Wind Speed Range: 0-70 m/s Resolution: 0.1 m/s Accuracy: 0 to 30 m/s, ±2% Wind Direction Range: 0-360 ° Resolution: 1 degree Accuracy: ± 2 degrees
Solar Radiation	Apogee Solar Radiation SP-110	Range: 0 – 1750 W/m^2 Range: 0 – 1750 W/m^2 Operating Environment: - 25 to 55 °C, 0 to 100% RH
Rainfall	Waterlog – H 340 Rain Gauge	Resolution: 0.0004 mm (@ 101.4 mm /hr) Rate: 0 to 635 mm/hr Operating Temperature: -0 to +60 °C
Evapotranspiration	Derived	FAO Penman Monteith Method

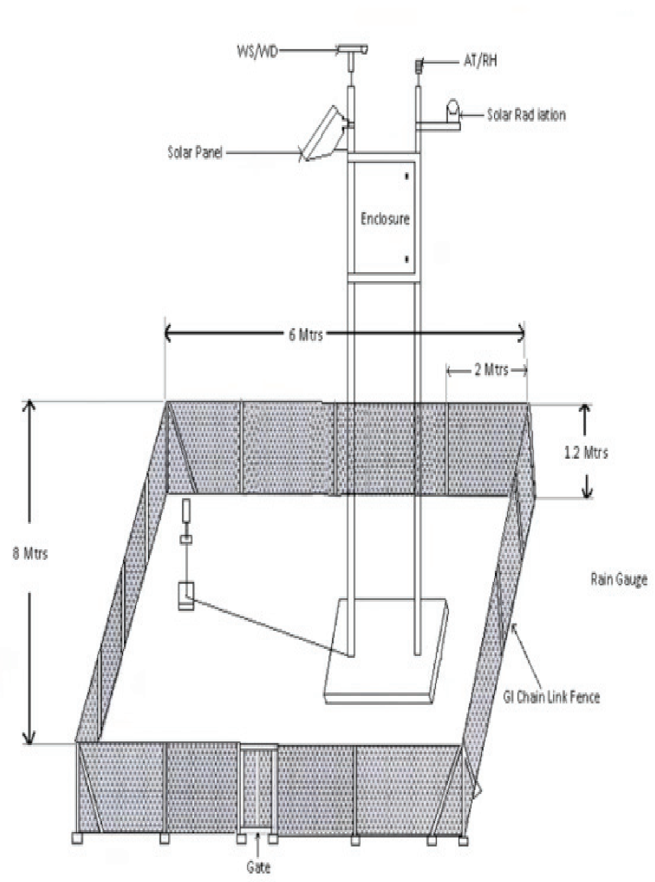

Fig.2: Civil drawing of the NICRA-AWS with fencing

5. Installation of NICRA AWS at different locations

The installation of the AWS at ICAR- CRIDA and the remaining 99 locations was completed by the mid of March 2012. The 99 locations include 11 stations in the north-eastern states, 2 locations in Jammu & Kashmir and one location in Andaman and Nicobar Islands. The KVK in-charge of respective stations were given the responsibility for safeguarding the stations, cleaning of the sensors and premises on regular basis. A glimpse of AWS installed at various locations is shown in **Fig.3**.

KVK, Kargil (J&K) – 2704m AMSL

KVK, Golaghat (Assam) – 95m AMSL

KVK, Aurangabad (Maharashtra) – 513m

KVK, Anantapur (AP) – 228m AMSL

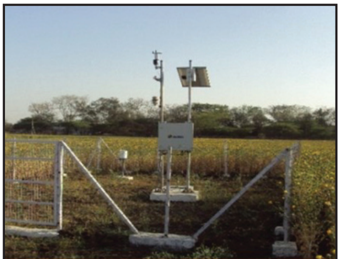

KVK, Raipur (Chhattisgarh) – 215m AMSL

KVK, Ranga Reddy (AP) – 536m AMSL

Fig.3: A glimpse of AWS installed at various locations

6. Flow of Data Under AWS Network

All the sensors are connected to a data logger to record, store and transmit data. The H-500XL Data logger is a standalone Data Collecting Platform (DCP) capable of communicating with Satellite, General Packet Radio Service (GPRS) / Global System for Mobile (GSM) modems, Telephone among other means of communication. The XL is ideal for small Hydrometeor logical systems. The data logger is connected to one GPRS Communication system, which transfers the data directly to the server installed at CRIDA. Sensors are scanned by the Data Logger for every 2 minutes interval. Data Logger log the scanned values from the sensors at every 30 minutes. Communication Modem transmits the logged values by the data logger for every 30 minutes Interval. File Transfer Protocol

(FTP) server at CRIDA receive the data through FTP and store the data in the respective folder. The data is made accessible to the public through the website (www.aicrpam-nicra-aws.in). Software Manager segregate the data and push the data to the web site to view the data online. The flow chart of NICRA-AWS network is shown in **Fig.4**.

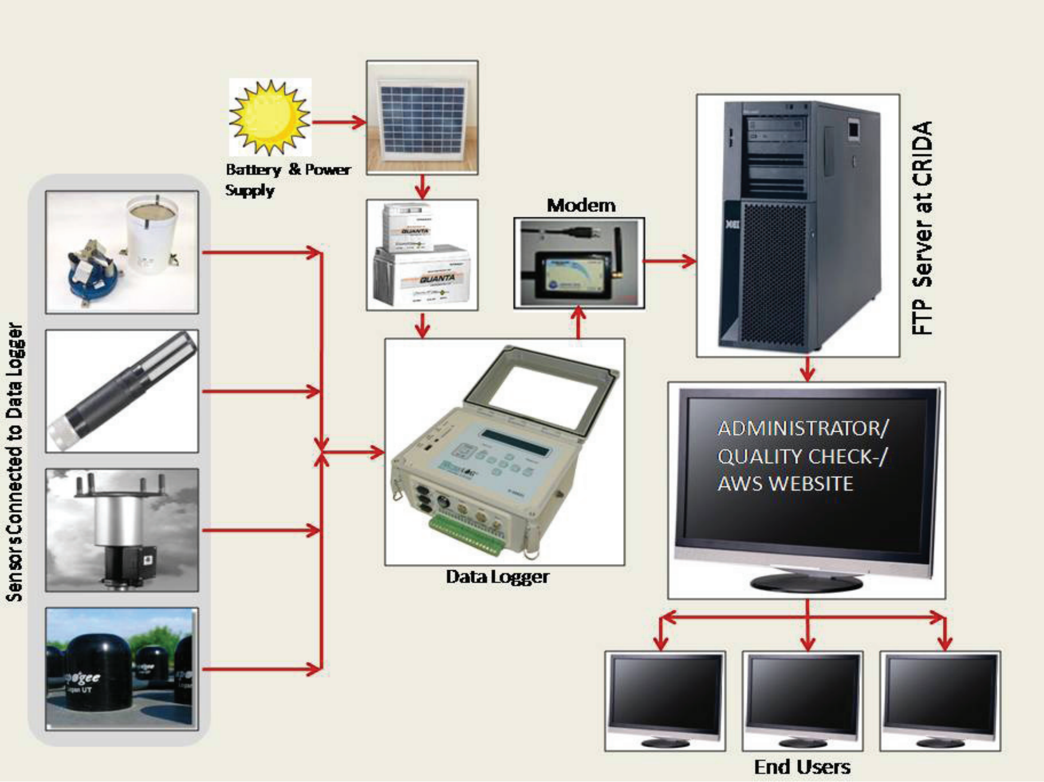

Fig.4: Flow chart of NICRA-AWS network

7. NICRA-AWS Website (www.aicrpam-nicra-aws.in)

The data from all 100 locations is made accessible through the website (www.aicrpam-nicra-aws.in) which started functioning from April 2012. The public can view the real time and past 24 hour observations from all the 100 locations by a click on the icon indicating each station on the Google map on the home page.

The access of data archives is restricted to institutions and organizations having username and password issued by AICRPAM only. However, the data from all 100 AWS locations are shared with some of the NICRA collaborating partners like Indian Agricultural Research Institute (IARI), New Delhi, Regional centers (Hyderabad and Chennai) of India Meteorological Department (IMD) etc. The local authorities of all the 100 AWSs are accessing the data archives of their respective locations through username and password provided to them. In addition to the 100 KVK users, nearly 200 registered users are regularly downloading and viewing the data. The public can register for getting data archives by filling the request form for new user registration and receive data after due approval from CRIDA authorities. The demand for weather data from NICRA-AWS network is high because of the better quality of the data without many missing values. A screen shot of the home page of the NICRA-AWS website with real time display of data is shown in **Fig.5** and **Fig.6,** respectively.

Fig.5: Home page of NICRA-AWS

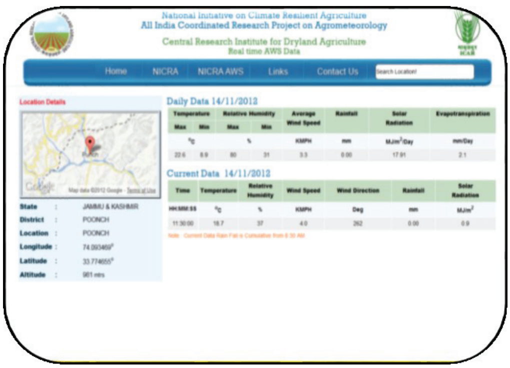

Fig.6: Real time display of AWS data

8. Quality Checking of AWS Data

The quality checking procedures are being applied to the data recorded from Automatic Weather Stations to monitor the quality of data prior to their use in computation of derived weather parameters. The quality checking intends to identify erroneous or anomalous data primarily to indicate any sensor malfunction, instability, interference in order to reduce the errors in data.

a. Credible Value Check

The aim of the check is to verify if the values of instantaneous data are within the acceptable range. Limits of different meteorological parameters depend on the season prevailing at the location. The values falling beyond these limits are scrutinized. Upper and lower limits of each weather parameter at a particular location for a given month are presented in **Fig.7**. In addition to the weather parameters, the maximum and minimum voltage levels of the battery is also displayed, irrespective of the station and day of the year. If the battery level goes below the minimum value (12 Volt), it is assumed that the station is going to stop transmitting the data to server in the next 2 days. The stoppage of the transmission is prevented at that particular location by recharging the battery so as to avoid any missing data.

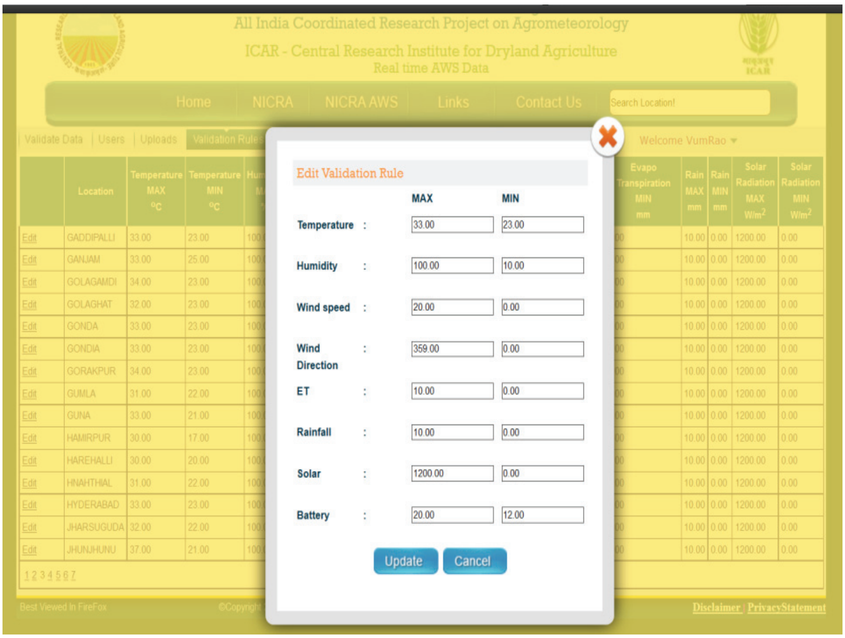

Fig.7: The module for data quality check in NICRA-AWS website

b. Comparing with previous observation

The aim of the check is to verify the abrupt change (unrealistic jumps in data). After each signal measurement, the current sample data is compared with the preceding one. If the difference of these two data sets is more than the specified limit then the current data set is identified as doubtful.

c. Comparing with manual observational data

For checking the credibility of the data, AWS data is compared with the available manual observational data by plotting 1:1 relationship. The validation of AWS data is done on an annual basis, wherever manually observed data is available. Scatter plot between AWS and manual data of maximum temperature (T_{max}), minimum temperature (T_{min}) and rainfall at various locations is shown in Fig.8.

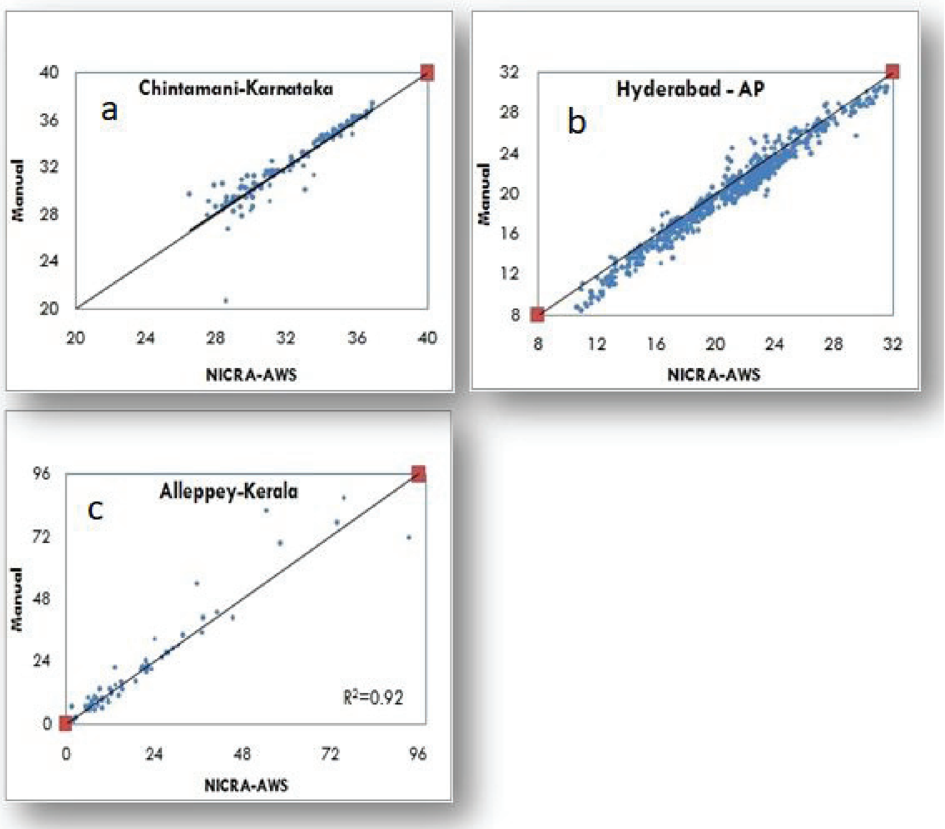

Fig.8: Scatter plot between NICRA-AWS recorded and manually observed data of (a) T_{max}, (b) rainfall and (c) T_{min} at different locations

d. AWS Data Calendar

The quality checking of the AWS data (both half-hourly and daily) is carried out on a daily basis to identify anomalous data at any location, if any. An AWS data calendar (**Fig.9**) is used for the quality checking and it is updated on daily basis for quick and easy monitoring of the data. All the data is flagged as Good, Sensor Issues, Doubtful/Suspect and Missing under different colours and alphabets assigned for operational ease. A daily report on AWS data is prepared and sent to the competent authority for rectification.

Date	Ranga Reddi	Anantapur	Khammam	Kurnool	Nalagonda	Srikakulam	Undi	Pedavagi	Ahmednagar	Amaravati	Aurangabad	Buldhana	Gondia	Nandurbar	Pune	NIASM	Ratnagiri	Kutchh	Rajkot	Valsad	Mangal Bharati	Anand	Bharatpur	Jhunjhunu	Jodhpur	Udaipur
19-Jun-13							W															S			W	
20-Jun-13							W				T											S				
21-Jun-13							W																			
22-Jun-13							W										S									
23-Jun-13							W										S									
24-Jun-13							W																			
25-Jun-13							W																			
26-Jun-13							W										S									
27-Jun-13							W										S									
28-Jun-13							W										S									
29-Jun-13							W										S									
30-Jun-13							W										S									
01-Jul-13							W										S									
02-Jul-13							W										S									
03-Jul-13							W										S						W			
04-Jul-13							W										S						W		W	
05-Jul-13							W										S						W		W	
06-Jul-13							W										S	H					W		W	
07-Jul-13							W										S	H					W		W	
08-Jul-13							W										S						W			
09-Jul-13							W										S	H					W			
10-Jul-13							W											H					W			
11-Jul-13							W											H								
12-Jul-13							W										S	H					W			
13-Jul-13							W										S	H								
14-Jul-13							W										S	H					W		W	

Quality Data		Temperature	T	Wind	W	Solar Radiation	S
Data Missing		Humidity	H	Rainfall	R	Evapotranspiration	E

Fig.9: Data calendar of NICRA-AWS

9. Utility of the AWS Data - Value added products

9.1 Monsoon Monitoring

Agricultural production in India is largely dependent on the performance of southwest monsoon, which brings about 80% of the total precipitation over the country. Changes in climate over the Indian region, particularly the southwest monsoon, would have a significant impact on agricultural production, water resources management and overall economy of the country. The climate change impacts are affecting the rhythm of monsoon, in particular the onset and withdrawal dates. The onset dates are likely to become earlier or not to change much while monsoon withdrawal dates are very likely get delayed, resulting in lengthening of the monsoon season (IPCC, 2013). The daily rainfall data from 100 NICRA-AWS locations are used in mapping and thereby knowing the progress and distribution of rainfall during the monsoon.

The total rainfall recorded during the months of June, July, August and September for the years 2012, 2013 and 2014 are compared with their respective district normal. The deviation of the rainfall at each NICRA-AWS from the IMD specified normal rainfall falls under any of the category viz, excess (20% or more), normal (-19% to +19%), deficient (-59% to -20%), scanty (-99% to -60%) and no rain (-100%). The deviation of actual rainfall with their normal at all the AWS are tabulated and interpolated maps are drawn (inverse distance method) using GIS environment. The maps have been compared with the sub-divisional rainfall deviation maps published by IMD maps every year, after the end of southwest monsoon season. The interpolated southwest monsoon rainfall deviation maps are showing similar pattern compared to IMD as shown in **Fig.10-12**. The low density of the NICRA-AWS doesn't represent the entire country and because of its uneven geographic distribution, the actual scenario of the southwest monsoon deviation is not portrayed well in the figures.

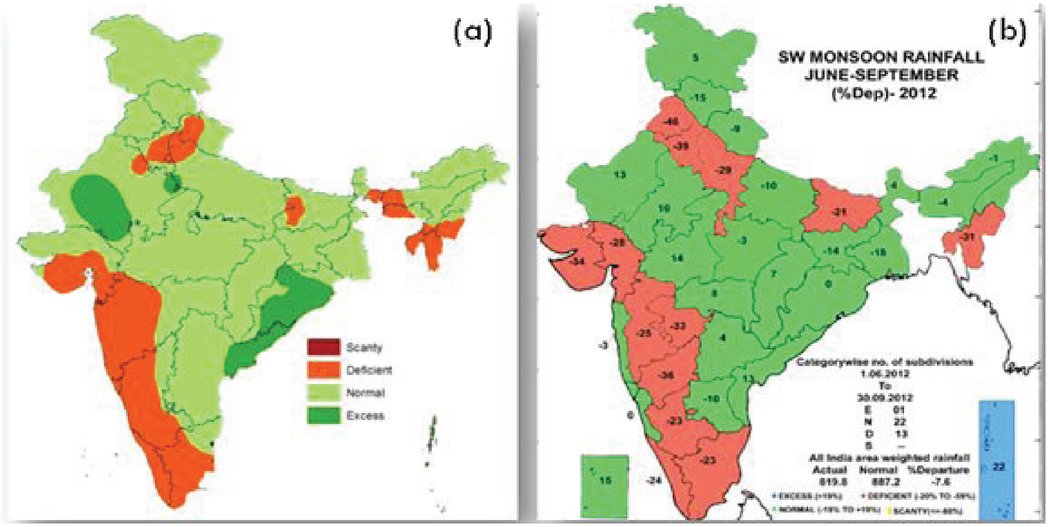

Fig.10: Southwest monsoon rainfall departure maps (2012) from long term normals using (a) NICRA-AWS rainfall data and (b) IMD rainfall data

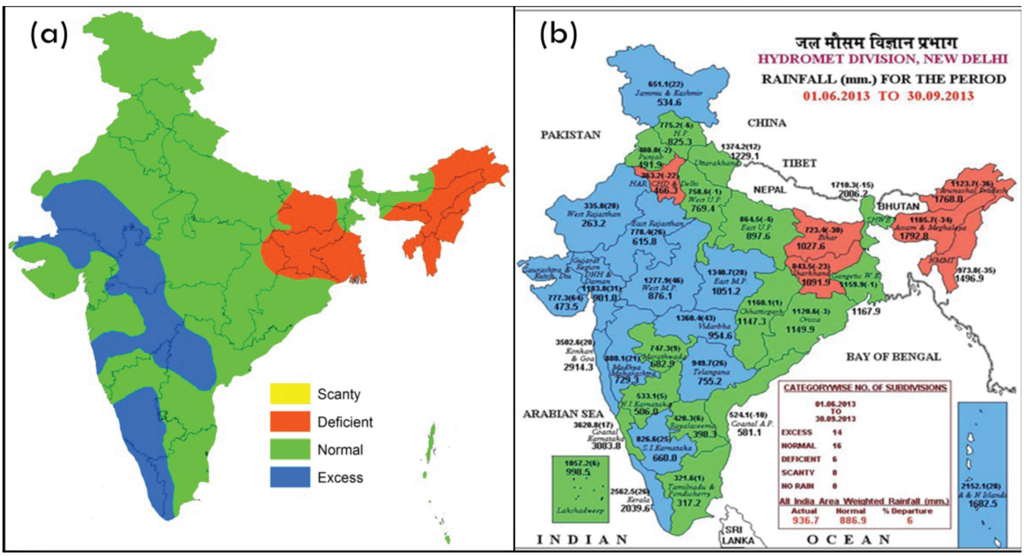

Fig.11: Southwest monsoon rainfall departure maps (2013) from long term normals using (a) NICRA-AWS rainfall data and (b) IMD rainfall data

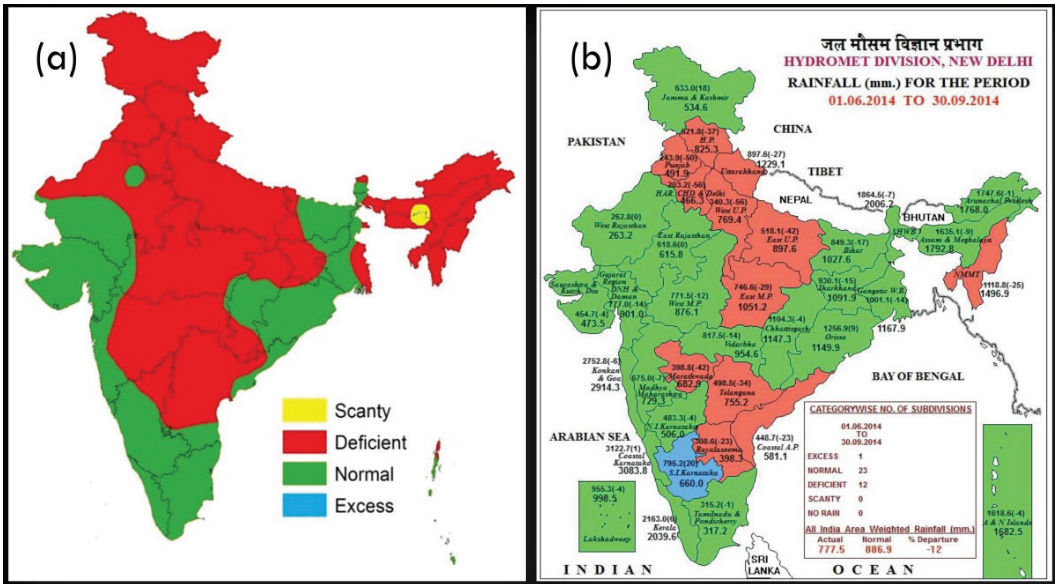

Fig.12: Southwest monsoon rainfall departure maps (2014) from long term normals using (a) NICRA-AWS rainfall data and (b) IMD rainfall data

9.2 Heat and Cold Wave Analysis

Since 1950, there has been a substantial increase in the number of heat waves worldwide and also, the heat waves have become longer in duration (Trenberth et al., 2007, 2012). The hottest days and nights have started to become hotter and more frequent (Gutowski et al., 2008). In the past several years, the global area hit by extremely unusual hot summer temperatures has increased fifty□folds (Hansen et al., 2012). It is now very likely that human influence has contributed to observed global scale changes in the frequency and intensity of daily temperature extremes since the mid-20th century, and likely that human influence has more than doubled the probability of occurrence of heat waves in large parts of Europe, Asia and Australia (IPCC, 2013).

Heat waves are a characteristic of summers in India. Heat waves are generally measured relative to the usual weather in the area and relative to normal temperatures for the season. The World Meteorological Organization (WMO) identifies a heat wave when the daily maximum temperature of more than five consecutive days exceeds the average maximum temperature by 5^0C, in a respective location. The heat wave phenomenon is part of the atmosphere's synoptic scale circulation. A heat wave occurs when a system of high pressure in the atmosphere moves into an area. In such a high-pressure system, air from upper levels of our atmosphere is pulled toward the ground, where it becomes compressed and increases in temperature.

India has witnessed increased incidence of heat waves in the recent past. The present study made an attempt to analyze the distribution of heat and cold waves all over the country during the summer and winter seasons, in the years 2013, 2014 and 2015 respectively using NICRA-AWS data. The departure of daily data from the long term normals of IMD has been used to identify heat/cold waves. If the daily maximum temperature is above 4.5 °C than the long term normal (IMD), it is identified as heat wave and if the daily minimum temperature is below 4.5 °C than long term normal (IMD), it is identified as cold wave. The total number of days falling in the above criteria over all the NICRA-AWS stations during the summer and winter seasons has been estimated and maps were generated using inverse distance weighted method in GIS environment and shown in **Fig.13** and **Fig.14**.

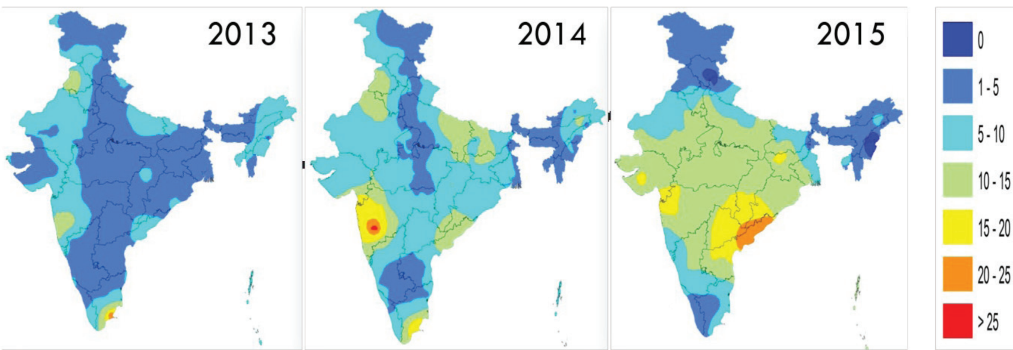

Fig.13: Number of days with heat wave conditions during summer season of 2013, 2014 and 2015

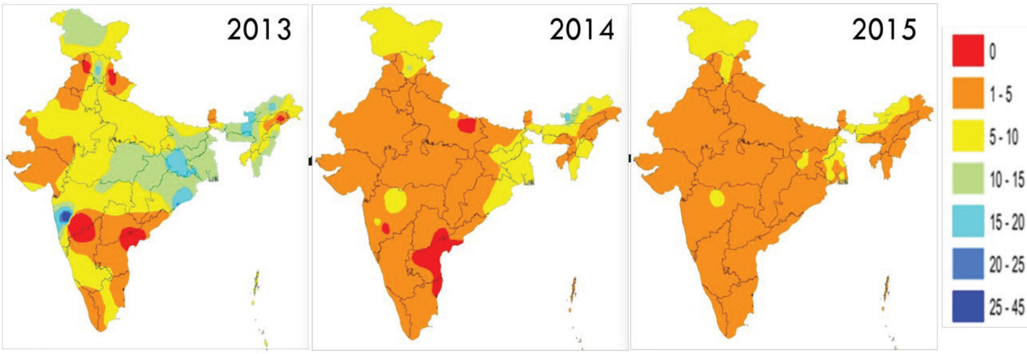

Fig.14: Number of days with cold wave conditions during winter season of 2013, 2014 and 2015

From the above maps it is clear that the heat wave during the summer 2015 is more intense and is distributed all over the country. The number of days with heat wave conditions were observed to be more during 2015 in comparison to 2013 and 2014. The maximum affected areas of heat wave2015 were observed in Odisha, Telangana, coastal Andhra Pradesh and Chhattisgarh regions which is clearly visible in the maps. In 2014, Marathwada and Madhya Maharashtra regions were mostly affected by heat wave.

The inter-comparison of cold waves during the winter season of 2013, 2014 and 2015 showed that more regions of the country was affected by cold wave during 2013 as compared to 2014 and 2015. Konkan and coastal Maharashtra, Madhya Maharashtra, east Madhya Pradesh, Jharkhand, Bihar, Odisha, West Bengal and most parts of northeastern States got affected by cold wave during winter 2013.

9.2.1 2015-Heat Wave - A Case Study

The summer 2015 heat wave is affected many regions in India and caused death of 2248 people across the country. An attempt has been made to quantify the intensity and duration of heat wave that resulted in high mortality across the country using Physiologically Equivalent Temperature (PET). PET is a thermal index based on a complete heat budget of the human body and includes both meteorological and thermo-physiological aspects (Mayer and Höppe, 1987; Höppe, 1999; Matzarakis et al., 1999). Half hourly PET, based on a complete heat budget of human body, was estimated using automatic weather station (AWS) data of four locations in Andhra Pradesh state, where the maximum numbers of death were reported. Ranges of PET in °C and related physiological stress and thermal perception is given in **Table 2**.

Table 2. PET ranges (°C) and related heat stress and thermal perception

PET (°C)	Heat stress	Thermal perception
< 4	Extreme cold stress	Very cold
4-8	Strong cold stress	Cold
8-13	Moderate cold stress	Cool
13-18	Slight cold stress	Slightly cool
18-23	No thermal stress	Comfortable
23-29	Slight heat load	Slightly warm
29-35	Moderate heat load	Warm
35-41	Strong heat load	Hot
> 41	Extreme heat load	Very Hot

The heat wave characterization using PET revealed that extreme heat load conditions (PET > 41) existed in all the four locations throughout May. The results of one location, named 'Undi' in West Godavari district is presented in **Fig.15.**

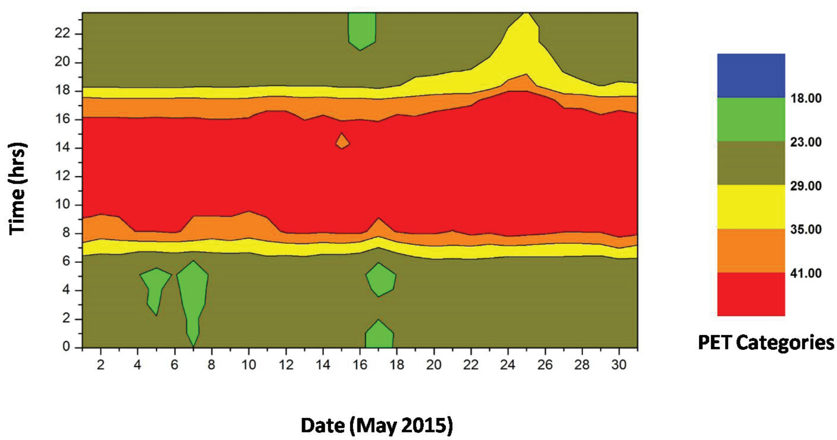

Fig.15: PET (°C) over Undi (West Godavari) during May 2015

The intensity and duration of heat waves was characterized by 'area under the curve' method. Area under the curve of PET > 41 °C and daily death rates indicated the relation between the two parameters Maximum number of daily death rates were reported when PET values exceeds 41 °C at Undi (**Fig.16**)

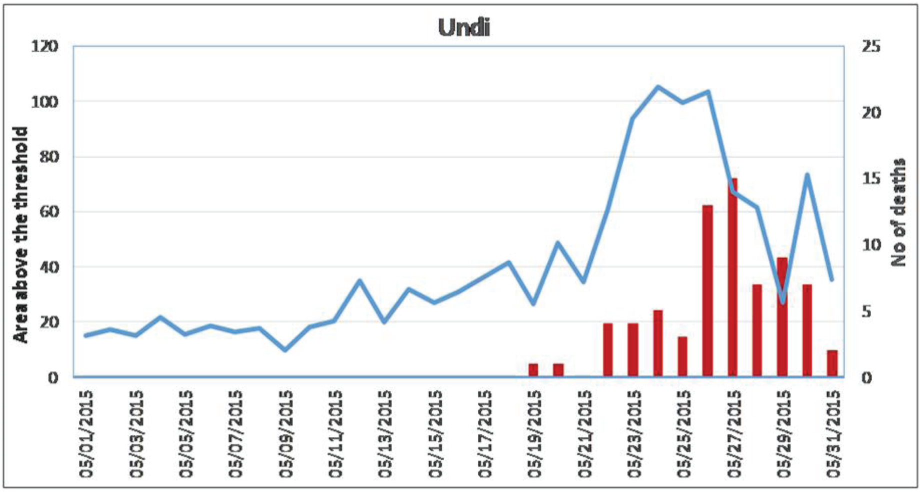

Fig.16: Area under the curve (PET >41) and daily death rate at Undi in May 2015

Such studies can be undertaken to identify heat wave prone areas of the country and to help in developing heat wave action plans and prioritization of activities for mitigating the adverse effects of heat waves.

9.3 Estimation of Solar Constants

Solar radiation (R_s), the primary energy source for all natural process that takes place on the Earth, is an important input parameter to many crop simulation models (DSSAT, Infocrop, APSIM etc), and also an inevitable factor for many applications, including evapotranspiration estimates, architectural design, and solar energy systems. Solar radiation is not widely measured due to the cost, maintenance and calibration requirements of the measuring instruments, despite its significance. In many days solar radiation data are missing or lie outside the expected range due to equipment failure and other problems (Hunt et al., 1998; Abraha and Savage, 2008) even at stations where solar radiation is measured. These limitations provided incite to the scientists to develop various models to estimate the solar radiation from other meteorological parameters, for the days or years when the data are missing, or for the locations where the data are not measured. The majority of the models developed by the scientists in estimating the solar radiation are based on the commonly measured meteorological parameters like maximum and minimum temperature, sunshine duration, precipitation, relative humidity, cloud cover etc.

In the present analysis, daily data on maximum and minimum temperature recorded by the NICRA-AWS at Kangra (32.1 °N, 76.3 °E, 733 m) location is used in calibrating, validating and comparing the existing models in predicting the solar radiation. The data from 1-Apr-2012 to 31-Mar-15 was used for calibrating the models whereas the data from 1-Apr-15 to 31-Dec-15 is used in validating the models.

9.3.1 Hargreaves and Samani Model

A simple equation to estimate daily solar radiation (R_s) from the diurnal range of air temperature was formulated by Hargreaves and Samani (1982)

$$R_s = R_a * a * \sqrt{\Delta T}$$

where R_a is the extraterrestrial radiation (MJ m^{-2} day^{-1}), 'a' is the empirical constant and $\Delta T = T_{max} - T_{min}$, where T_{max} and T_{min} are the maximum and minimum temperature of the day, respectively. Many scientists later modified this model by adding an extra empirical constant to the base model. **Table 3** shows the Hargreaves-Samani (H-S) model and its modified versions which were used in the present study.

Table 3: Hargreaves-Samani and its modified models

Model	Empirical Relation
Hargreaves-Samani (1982)	$R_s = R_a * a * \sqrt{\Delta T}$
Hargreaves et al. (1985)	$R_s = R_a * a * \sqrt{\Delta T} + \text{b}$
Annandale et al. (2002)	$R_s = R_a * a * (1 + 2.7 * 10^{-5} * z) * \sqrt{\Delta T}$
Chen et al. (2004)	$R_s = R_a * (a * \sqrt{\Delta T} + \text{b})$

z - altitude of the location

9.3.2 Bristow-Campbell Model

Using the same data that was used in Hargreaves-Samani model, Bristow and Campbell (1984) developed a relationship between atmospheric transmittance and a daily range of air temperature in estimating the daily global solar radiation, which is written as the following relation

$$R_s = R_a * a * (1 - \exp(-b * \Delta T^c))$$

where ΔT is the daily range of air temperature; and a, b and c are empirical coefficients, determined for a particular location from measured solar radiation data. Like Hargreaves-Samani model, Bristow-Campbell was also modified many times. The Bristow-Campbell (B-C) model and its modified versions used in the present analysis are shown in **Table 4**.

Table 4: Bristow-Campbell and its modified forms

Model	Empirical Relation
Bristow-Campbell (1984)	$R_s = R_a * a * (1 - \exp(-b * \Delta T^c))$
Donatelli-Campbell (1998)	$R_s = R_a * a * (1 - \exp(-b * (\frac{\Delta T^c}{T_m})))$
Goodin et al. (1999)	$R_s = R_a * a * (1 - \exp(-b * (\frac{\Delta T^c}{R_a})))$
Meza-Varas (2000)	$R_s = R_a * 0.75 * (1 - \exp(-b * \Delta T^2))$
Weiss et al. (2001)	$R_s = R_a * 0.75 * (1 - \exp(-b * (\frac{\Delta T^2}{R_a})))$
Abraha-Savag (2008)	$R_s = R_a * 0.75 * (1 - \exp(-b * (\frac{\Delta T^2}{T_m})))$

T_m - monthly mean temperature

9.3.3 Statistical evaluation

The empirical coefficients contained in Hargreaves-Samani, Bristow-Campbell and their modified versions were determined using the Data fit (version 9.0) software. The measured and estimated global solar radiation by different models data were compared using Root Mean Square Error (RMSE), D-index and Normalised Orthogonal Function (NOF) (Ahuja et al., 2002). The RMSE between the simulated and observed values for a dataset with n measured points is defined as

$$RMSE = \sqrt{\sum_{i=1}^{n} \frac{(S_i - Ob_i)^2}{n}}$$

where S_i and Ob_i are the model estimated and measured values, respectively. The D-index is defined as

$$D = 1 - \frac{\sum_{i=1}^{n}(S_i - Ob_i)^2}{\sum_{i=1}^{n}(|S_i - Ob_{avg}| + |Ob_i - Ob_{avg}|)^2}$$

where Ob_{avg} is the average of the observed values. The D-index is a measure of the deviation between model estimates and observed in relation to the scattering of the observed data. It has a value ranging from 0 to 1, where D=1 means a perfect estimation. The normalized orthogonal function is defined as

$$NOF = RMSE/Ob_{avg}$$

NOF=0 indicates a perfect match between measured and estimated radiation. NOF < 1 may be interpreted as simulation error of less than one standard deviation around the experiment mean.

9.3.4 Calibration and Validation of H-S, B-C and its Modified Models

The models used for estimating global solar radiation require calibration. For that reason it is necessary to choose appropriate model the model coefficients to obtain a better fit between observed and estimated global solar radiation. The empirical coefficients of the model can be determined using observed solar radiation data. The coefficients of the various models determined using the Data-fit software is shown in **Table 4**. The estimation of global solar radiation can be made with an acceptable accuracy using all the tested calibrated models. The models were validated by comparing calculated and measured solar radiation at Kangra location. The statistical results of the different models are given in **Table 5**.

The statistical analysis shows that the solar radiation estimated using Hargreaves-Samani method and its modified version was found to be in good agreement with the observed values. All these models showed a high D-Index value of 0.94 with varying RMSE and NOF values. On the other hand, the models based on Bristow-Campbell and its modified forms gives a varying results in which the D-index varies from 0.74 to 0.96. In general, among the 10 models validated, Donatelli-Campbell model (a modified version of Bristow-Campbell) gives good result in terms of high D-Index value (0.96) and low RMSE (2.58 MJ m^{-2} day^{-1}) and NOF (0.20) values. This implies that, Donatelli-Campbell model can be used with confidence in estimating the solar radiation at Kangra location.

Table 5: Comparison of empirical constants calculated by different models

Empirical Models	Empirical Constant	Statistics		
		RMSE	D-Index	NOF
Hargreaves-Samani (1982) $R_s = R_a * a * \sqrt{\Delta T}$	a=0.11	3.15	0.94	0.25
Hargreaves (1985) $R_s = R_a * a * \sqrt{\Delta T} + b$	a=0.17 b=-6.48	3.41	0.94	0.27
Annandale (2002) $R_s = R_a * a * (1 + 2.7 * 10^{-5} * z) * \sqrt{\Delta T}$	a=0.11	3.12	0.94	0.24
Chen (2004) $R_s = R_a * (a * \sqrt{\Delta T} + b)$	a=0.17 b=0.21	3.03	0.94	0.24
Bristow-Campbel $R_s = R_a * a * (1 - \exp(-b * \Delta T^c))$	a=0.63 b=0.04 c=1.29	2.94	0.95	0.23
Donatelli-Campbell $R_s = R_a * a * (1 - \exp(-b * (\frac{\Delta T^c}{T_m})))$	a=0.51 b=0.07 c=2.24	2.58	0.96	0.20
Goodin $R_s = R_a * a * (1 - \exp(-b * (\frac{\Delta T^c}{R_a})))$	a=0.44 b=0.14 c=2.63	3.00	0.95	0.24
Meza-Varas $R_s = R_a * 0.75 * (1 - \exp(-b * \Delta T^2))$	b=0.01	6.18	0.74	0.48
Weiss $R_s = R_a * 0.75 * (1 - \exp(-b * (\frac{\Delta T^2}{R_a})))$	b=0.10	5.66	0.86	0.44
Abraha-Savag $R_s = R_a * 0.75 * (1 - \exp(-b * (\frac{\Delta T^2}{T_m})))$	b=0.05	3.33	0.94	0.26

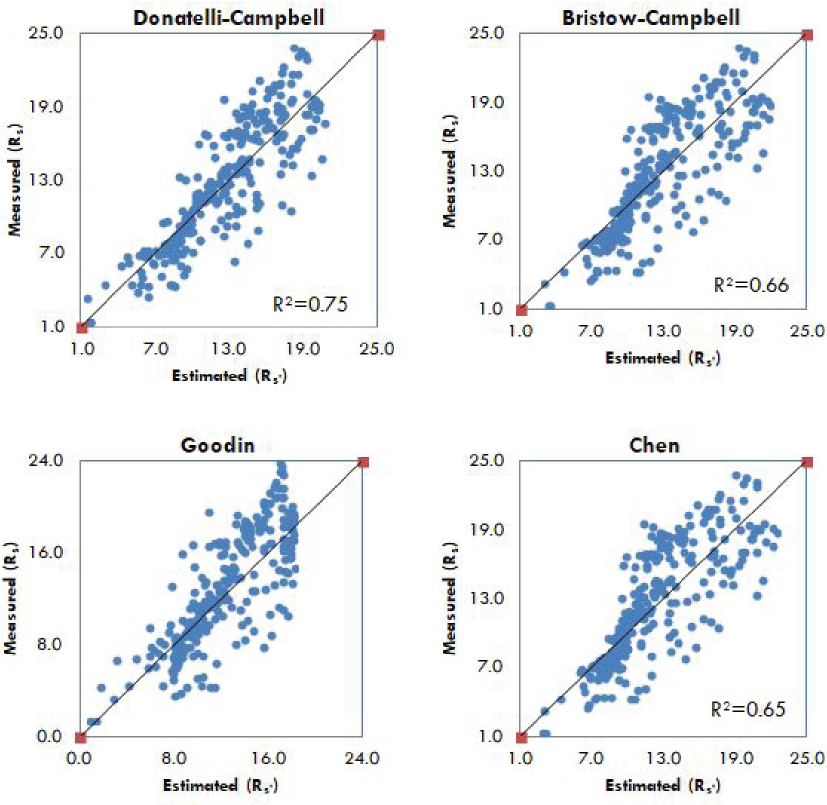

Fig.17: Scatter plot between measured and estimated solar radiation using different methods

Fig.17 shows the scatter plot between estimated and measured solar radiation using various methods. The same methodology can be employed to determine the best model in estimating solar radiation at the remaining 99 locations by calibrating and validating the models.

9.4 Monitoring of Nilam Cyclone Using NICRA-AWS data

Nilam cyclone was the first cyclone to hit the east coast of India after the installation of 100 AWS across the country. The effect of the cyclone was felt on meteorological data recorded at the AWS that was falling in the track of cyclone. The cyclone 'Nilam' has stuck the eastern coast of the country during the period

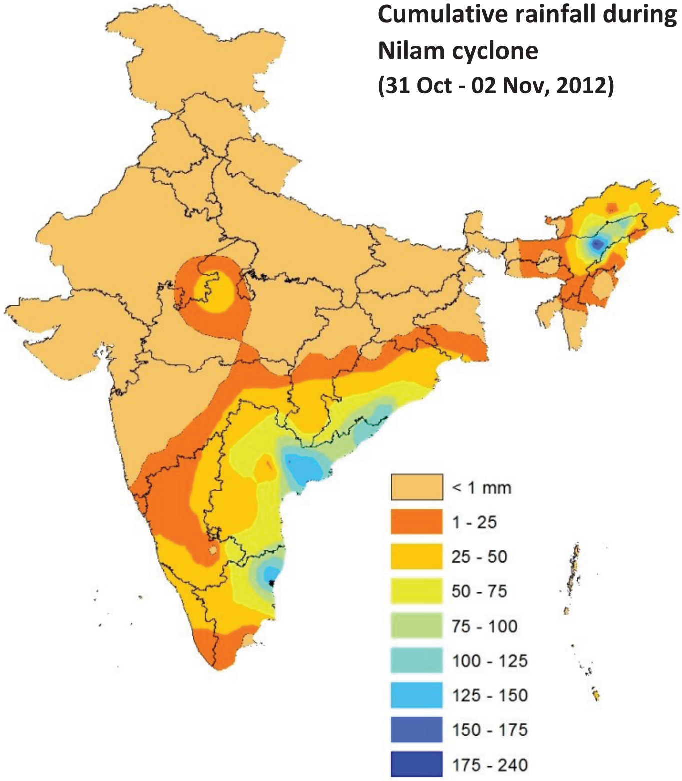

Fig.18: The spatial interpolation of cumulative rainfall during Nilam cyclone

31st October to 2nd November 2012. The stations located at eastern coast of Andhra Pradesh, Odisha and Tamil Nadu experienced heavy rainfall between 120-240 mm during this period. The spatially interpolated cumulative rainfall map during this period was prepared by using NICRA AWS data and is shown in **Fig.18**.

The daily variation in maximum temperature, rainfall and solar radiation for the AWS located at Tindivanam and Namakkal in Tamil Nadu;, Chintamani in Karnataka, Hyderabad and Wyra in Telangana and Anantapur, Pedavegi and Amadalavalasa in Andhra Pradesh due to the influence of 'Nilam' cyclone are depicted in the **Fig.19**. From this figure, it is observed that there is a sharp decrease in maximum temperature and solar radiation during the period 31st Oct to 2nd Nov, 2012.

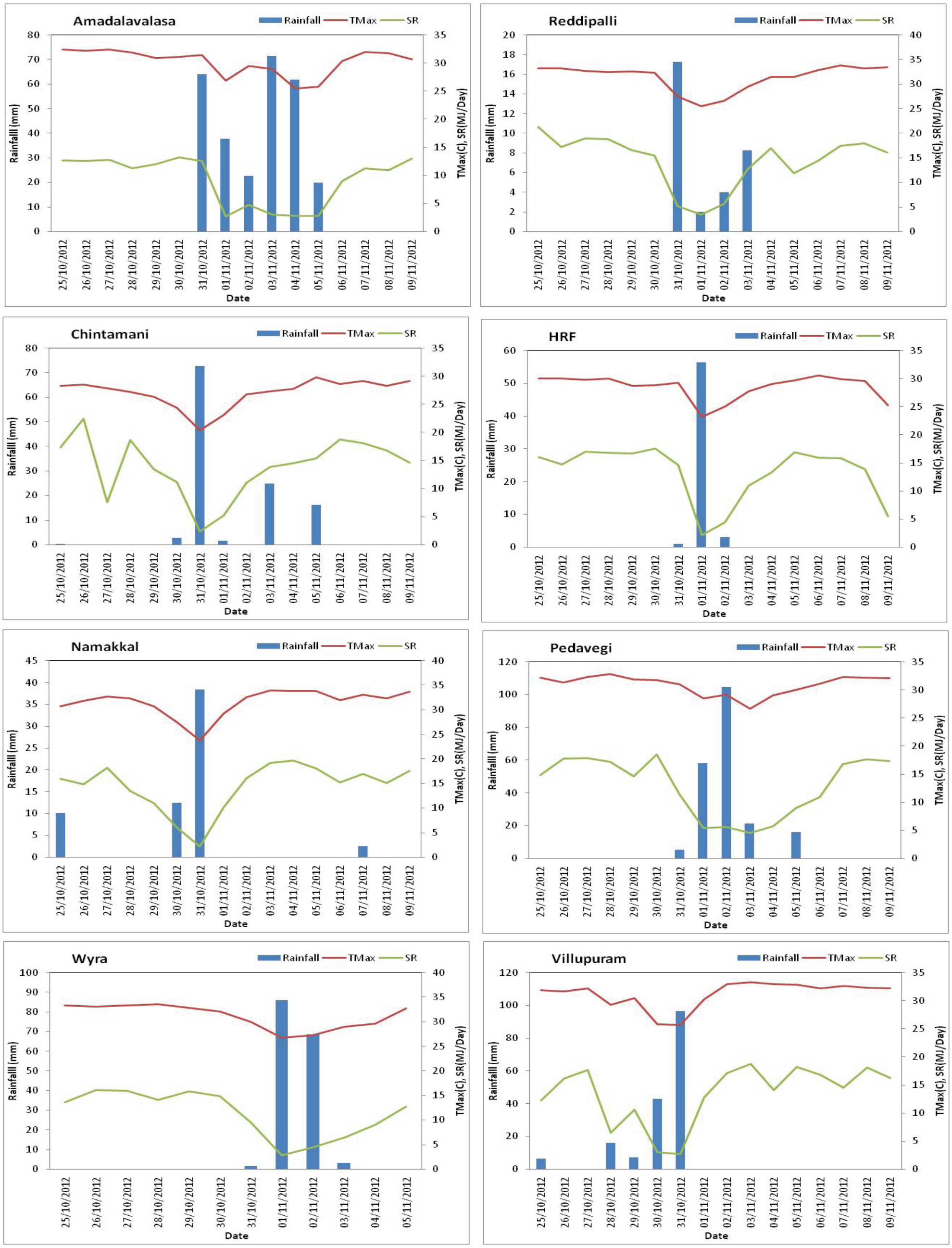

Fig.19: Change in weather parameters across some AWS located in the effected states during the Nilam cyclone

10. Way Forward

The surface meteorological observation plays a key role in understanding the spatial and temporal distribution of weather and climate. Need has been felt by India Meteorological Department since long to have continuous weather monitoring, particularly of remote/inaccessible places including river catchment areas and snow bound mountains. The network of AWS under IMD was started in this regard and many organizations like Indian Space Research Organization (ISRO), State Disaster Monitoring Cell of each State, various Non-Governmental Organizations (NGO) and other private agencies are having their own small and large network of AWS. ICAR also joined the list of AWS networks through establishment of AWS under NICRA which started functioning since April 2012. Within this short span of time, NICRA-AWS has got wide acceptance and recognition among the scientific community, farmers and other stake holders. Providing quality data without many missing values makes the NICRA-AWS distinguished from other networks. Apart from the daily data, NICRA-AWS is also providing half-hourly data of each location. The success of the NICRA-AWS is mainly because of the continuous monitoring of the half-hourly data of each location by a dedicated team of AICRP on Agrometeorology at ICAR-CRIDA.

However, the NICRA-AWS network needs to be expanded, as more KVK's, research stations and institutes are requesting to install the AWS. Apart from downloading the daily and half-hourly data, the AWS website needs to be upgraded by adding more features viz., comparing the actual data with normal's, graphical representation of the weather variables etc. The security of the stations is a big concern, though all 100 stations were installed within the KVK campus. Theft of solar panel, sensors and even data logger as a whole were reported from few stations. Therefore, as an advanced precaution, the AWS stations needs to be insured against theft cases. In addition to these measures, calibration of each sensor needs to be carried out twice in a year.

REFERENCES

Abraha, M.G. and Savage, M.J. (2008). Comparison of estimates of daily solar radiation from air temperature range for application in crop simulations. *Agricultural and Forest Meteorology 148*: 401-416.

Ahuja, L.R., Ma, L. and Howell, T.A. (2002). Agricultural system models. Field Research and Technology Transfer. CRC press. New York, USA.

Alory, G., Wijffels, S. and Meyers, G. (2007). Observed temperature trends in the Indian Ocean over 1960–1999 and associated mechanisms, *Geophysical Research Letters*, 34 (2).

Bapuji Rao, B., Santhibhushan C. P., Sandeep, V.M., Pramod, V.P. and Rao, V.U.M. (2014). Spatial analysis of the sensitivity of wheat yields to temperature in India. *Agricultural and Forest Meteorology* 200 (2015): 192–202.

Battisti, D.S. and Naylor R.L. (2009), Historical warnings of future food insecurity with unprecedented seasonal heat. *Science*, 323(5911): 240–244.

Bristow, C.L. and Campbell, G.S. (1984). On the relationship between incoming solar radiation and daily maximum and minimum temperature. *Agricultural and Forest Meteorology*, 31:159-166.

Brown, M. and Christopher, C.F. (2008). Food Security Under Climate Change. Science (New York, N.Y.). 319. 580-1. 10.1126/science.1154102. Donatelli, M. and Campbell, G.S. (1998). A simple model to estimate global solar radiation. In: Proc. ESA Congress, 5th, Nitra, Slovak Republic, pp. 133-134

Easterling, D.R., Horton, B., Jones, P.D., Peterson, T.C., Karl, T.R., Parke, D.E. (1997). Maximum and minimum temperature trends for the globe, *Science* 277 (5324): 364–367.

Fischer, G., Shah, M., Tubiello F.N. and Van Velhuizen H. (2005). Socio-economic and climate change impacts on agriculture: an integrated assessment, 1990–2080, Philos. *Transactions of Royal Society B Biological Sciences* 360(1463): 2067–2083.

Goodin, D.G., Hutchinson, J.M.S., Vanderlip, R.L. and Knapp, M.C. (1999). Estimating solar irradiance for crop modeling using daily air temperature data. *Agronomy Journal* 91, 845-851.

Gutowski, W.J., Hegerl, G.C., Holland, G.J., Knutson, T.R., Mearns, L.O., Stouffer, R.J., Webster, P.J., Wehner, M.F. and Zwiers, F.W. (2008). Causes of Observed Changes in Extremes and Projections of Future Changes in *Weather and Climate Extremes in a*

Changing Climate. Regions of Focus: North America, Hawaii, Caribbean, and U.S. Pacific Islands. T.R. Karl, G.A. Meehl, C.D. Miller, S.J. Hassol, A.M. Waple, and W.L. Murray (eds.). A Report by the U.S. Climate Change Science Program and the Subcommittee on Global Change Research, Washington, DC.

Hansen, J., Sato, M. and Ruedy, R. (2012). Perceptions of Climate Change: The New Climate Dice. Submitted for publication to the *Proceedings of the National Academy of Science, PNAS*. http://arxiv.org/abs/1204-1286.

Hargreaves, G.H. and Samani, Z.A. (1982). Estimating potential evapotranspiration. *Journal of Irrigation and Drainage Engineering, ASCE,* 108(IR3): 223-230.

Höppe, P. (1999). The physiological equivalent temperature — a universal index for the biometeorological assessment of the thermal environment. *International Journal of Biometeorology* 43 (2), 71–75.

Hunt, L.A., Kucharb, L. and Swanton, C.J. (1998). Estimation of solar radiation for use in crop modeling. *Agricultural and Forest Meteorology* 91: 293-300.

IPCC (2013). Climate Change 2013: The Physical Science Basis. Contribution of Working Group I to the Fifth Assessment Report of the Intergovernmental Panel on Climate Change [Stocker, T.F., D. Qin, G.K. Plattner, M. Tignor, S.K. Allen, J. Boschung, A. Nauels, Y. Xia, V. Bex and P.M. Midgley (eds.)]. Cambridge University Press, Cambridge, United Kingdom and New York, NY, USA, 1535 pp.

Karl, T.R., Knight, R.W., Easterling, D.R. and Quayle, R.G. (1996). Indices of Climate Change for the United States, *Bulletin of American Meteorological Society* 77(2): 279–292.

Lobell, D.B. and Asner, G.P. (2003). Climate and management contributions to recent trends in US agricultural yields, *Science* 299(5609): 1032–1032.

Lobell, D.B. and Field, C.B. (2007). Global scale climate–crop yield relationships and the impacts of recent warming, *Environmental Research Letters* 2(1): 014002.

Lobell, D.B., Burke, M.B., Tebaldi, C., Mastrandrea, M.D., Falcon, W.P. and Naylor, R.L. (2008). Prioritizing climate change adaptation needs for food security in 2030, *Science* 319(5863): 607–610.

Matzarakis, A., Mayer, H. and Iziomon, M.G. (1999). Applications of a universal thermal index: physiological equivalent temperature. *International Journal of Biometeorology* 43(2): 76–84.

Mayer, H. and Höppe, P. (1987). Thermal comfort of man in different urban environments. *Theoretical and Applied Climatology* 38(1): 43–49.

Meza, F. and Varas, E. (2000). Estimation of mean monthly solar global radiation as a function of temperature. *Agricultural and Forest Meteorology* 100: 231-241.

Mishra, V. and Cherkauer, K.A. (2010). Retrospective droughts in the crop growing season: Implications to corn and soybean yield in the Midwestern United States, *Agricultural and Forest Meteorology* 150(7): 1030–1045.

Mishra, V., Smoliak, B.V., Lettenmaier, D.P. and Wallace, J.M. (2012). A prominent pattern of year-to-year variability in Indian Summer Monsoon Rainfall, *Proceedings of National Academy of Sciences* 109(19): 7213–7217, doi:10.1073/pnas.1119150109.

Mishra, V., Kumar, D., Ganguly, A., Sanjay, J., Mujumdar, M., Krishnan, R. and Shah, D.R. (2014a). Reliability of regional and global climate models to simulate precipitation extremes over India. *Journal of Geophysical Research Atmosphere* 119, doi:10.1002/2014JD021636.

Mishra, V., Shah, R. and Thrasher, B. (2014b). Soil Moisture Droughts under the Retrospective and Projected Climate in India, *Journal of Hydrometeorology*, 141006071153004, doi:10.1175/JHM-D-13-0177.1.

Schmidhuber, J. and Tubiello, F.N. (2007). Global food security under climate change, *Proceedings of National Academy of Sciences* 104(50): 19703–19708.

Trenberth, K.E., Jones, P.D., Ambenje, P., Bojariu, R., Easterling, D., KleinTank, A., Parker, D., Rahimzadeh, F., Renwick, J.A., Rusticucci, M., Soden, B. and Zhai, P. (2007). Observations: Surface and Atmospheric Climate Change in *Climate Change 2007: The Physical Science Basis. Contribution of Working Group to the Fourth Assessment Report of the Intergovernmental Panel on Climate Change* (*Solomon, S.,D. Qin, M. Manning, Z.* Chen, M. Marquis, K.B. Averyt, M. Tignor and H.L. Miller(eds.). Cambridge University Press, Cambridge, United Kingdom and New York, NY, USA.

Trenberth, K.E., Meehl, J., Masters, J. and Richards, S. (2012). Heat Waves and Climate Change: A Science Update from Climate Communication. In: Climate Outreach; June 28, 2012 13pp

World Meteorological Organization (1992). *The WMO Automatic Digital Barometer Inter comparison: Final Report* (J.P. van der Meulen). Instruments and Observing Methods Report No. 46, (WMO/TD-No. 474), Geneva.

World Meteorological Organization (2005). Report of the meeting of the implementation coordination team on climate change/variability and natural disasters in agriculture, Commission for Agricultural meteorology, WMO, Geneva, Auckland, New Zealand.

ANNEXURE

Location of Automatic Weather Stations installed under NICRA

State	District	Agro-ecological Region	Climatic Hazard
Zone-I			
Himachal Pradesh (SAU)	Chamba	Mid Hills Sub-humid Zone (HP-2)	Cold Wave/ Drought /Frost
Himachal Pradesh (SAU)	Hamirpur	Sub-Montane & low hills, Sub-Tropical Zone (HP-1)	Drought
Himachal Pradesh (SAU)	Kinnaur	High hills Temperate Dry Zone (HP-4)	Cold Wave/ Drought
Himachal Pradesh (SAU)	Kullu	High Hills Temperate Wet Zone (HP-3)	Drought / Cold Wave
Himachal Pradesh (SAU)	Sirmaur	Western Himalayas (Warm Sub-humid)	Cold Wave
Himachal Pradesh (SAU)	Mandi	Western Himalayas (Warm Sub-humid)	Cold Wave
Himachal Pradesh (SAU)	Kangra	Western Himalayas (Warm Sub-humid)	Frost
Himachal Pradesh (SAU)	Kinnaur	High hills Temperate Dry Zone (HP-4)	Cold Wave/ Drought
Punjab (SAU)	Faridkot	Western Plain Zone (PB-4)	High Temperature
Jammu & Kashmir (SAU)	Poonch	Western Himalayas (Warm Sub-humid)	Cold Wave
Jammu & Kashmir (SAU)	Kargil	Western Himalayas (Cold Arid)	Frost
Zone-II			
Andaman & Nicobar Islands (ICAR)	Port Blair	Coastal Zone	Cyclone
Bihar (SAU)	Aurangabad	South Bihar Alluvial Plain zone (B1-3)	Drought
Bihar (ICAR)	Buxar	South Bihar Alluvial Plain zone (BI-3)	Drought/Flood

State	District	Agro-ecological Region	Climatic Hazard
Bihar (NGO)	Nawadah	South Bihar Alluvial Plain Zone (B1-3)	Drought
Bihar (SAU)	Saran	North West Alluvial Plain Zone (BI-1)	Flood/Drought
Bihar (SAU)	Supaul	North east Alluvial Plain Zone (BI-2)	Drought/Flood
Bihar (SAU)	Madhubani	Eastern Plain	Drought
Bihar (ICAR)	Muzaffarpur	Eastern Plain	Drought
Jharkhand (SAU)	Chatra	Western Plateau Zone (BI-5)	Drought/ Heat Wave
Jharkhand (NGO)	Gumla	Western Plateau Zone (BI-5)	Drought/ Heat Wave
Jharkhand (ICAR)	Koderma	Central and North Eastern Plateau Zone (B1-4)	Drought
Jharkhand (SAU)	Palamau	Western Plateau Zone (B1-5)	Drought/ Heat Wave
West Bengal (SAU)	Coochbehar	Terai Zone (WB-2)	Heavy Rainfall
West Bengal (SAU)	Malda	Old Alluvial Zone (WB-3)	Flood
Zone-III			
Arunachal Pradesh (State Govt.)	Tirap	Humid Subtropical Zone	Flood
Arunachal Pradesh (State Govt.)	West Kameng	Temperate Zone	Cold Stress
Arunachal Pradesh (ICAR)	West Siang	Sub Tropical Zone	Cold Stress
Assam (SAU)	Dibrugarh	Upper Bhramaputra Valley Zone (AS-2)	Flood
Assam (SAU)	Golaghat	Mid Bhramaputra Valley Zone (AS-2)	Flood
Manipur (CAU)	Imphal East	Mild Tropical Hill Zone	Drought

State	District	Agro-ecological Region	Climatic Hazard
Manipur (NGO)	Senapati	Sub Tropical Plain Zone	Drought
Meghalaya (ICAR)	Umaim	Mid Tropical Hill Zone	Drought
Mizoram (State Govt.)	Lunglei	Sub Tropical Hill Zone	Flood
Nagaland (State Govt.)	Mokokchung	High Hills Zone	Drought
Nagaland (ICAR)	Phek	High Hills Zone	Drought
Sikkim (ICAR)	East Sikkim	Humid Sub Tropical Zone	Soil Erosion/ Water Stress
Tripura (NGO)	West Tripura	Mid Tropical Plain Zone	Cyclone
Zone-IV			
Uttar Pradesh (SAU)	Baghpat	Western Plain Zone	Ground Water Depletion
Uttar Pradesh (SAU)	Behraich	Central Plain Zone (UP-6)	Flood
Uttar Pradesh (NGO)	Chitrakoot	Bundelkhand zone	Drought/ Heat Wave
Uttar Pradesh (NGO)	Gonda	Central Plain Zone	Flood
Uttar Pradesh (SAU)	Gorakhpur	North Eastern Plain Zone	Flood
Uttar Pradesh (SAU)	Hamirpur	Bundelkhand zone	Drought/ Heat Wave
Uttar Pradesh (ICAR)	Kushinagar	North Eastern Plain Zone (UP-8)	Flood
Uttar Pradesh (SAU)	Maharajganj	North Eastern Plain Zone	Flood
Uttar Pradesh (SAU)	Muzaffarnagar	Western Plain Zone	Ground Water Depletion
Uttar Pradesh (SAU)	Ramabainagar	Northern Plain and Central Highland	Drought
Uttar Pradesh (SAU)	Sonbhadra	Vindhyan Zone	Drought/ Heat Wave

State	District	Agro-ecological Region	Climatic Hazard
Uttarakhand (SAU)	Tehri Garhwal	Hill Zone (UP-1)	Cold Wave/ Hail Storm
Uttarakhand (ICAR)	Uttarkashi	Hill Zone (UP-1)	Cold Wave/ Flood/Hail Storm
Zone-V			
Andhra Pradesh (ICAR)	Ranga Reddy	Deccan Plateau and Eastern Ghats	Drought
Andhra Pradesh (SAU)	Anantapur	Scarce rainfall zone (AP-3)	Drought
Andhra Pradesh (SAU)	Khammam	High altitude and tribal area zone (AP-7)	Drought/ Heat Stress
Andhra Pradesh (NGO)	Kurnool	Scarce rainfall zone (AP-3)	Drought
Andhra Pradesh (NGO)	Nalgonda	Southern Telangana zone (AP-4)	Drought
Andhra Pradesh (SAU)	Srikakulam	Northern coastal zone (AP-2)	Flood
Andhra Pradesh (SAU)	West Godavari	Krishna Godavari zone (AP)	Cyclone
Andhra Pradesh (ICAR)	West Godavari	Krishna Godavari zone (AP)	Cyclone
Maharashtra (NGO)	Ahmednagar	Western Ghat zone (MH-3)	Drought
Maharashtra (NGO)	Amaravati	Central Maharashtra Plateau Zone (MH-7)	Central Plateau
Maharashtra (SAU)	Auranagabd	Scarcity zone (MH-6)	Drought
Maharashtra (SAU)	Buldhana	Deccan Plateau (Hot Sem-Arid)	Drought
Maharashtra (SAU)	Gondia	Eastern Vidarbha zone (MH-9)	Drought
Maharashtra (NGO)	Nandurbar	Western Maharashtra plain zone (MH-5)	Drought/ Heat Stress
Maharashtra (NGO)	Pune	Western Maharashtra plain zone (MH-5)	Drought

State	District	Agro-ecological Region	Climatic Hazard
Maharashtra (SAU)	Ratnagiri	South Konkan Coastal Zone (MH-1)	Flood
Maharashtra (ICAR)	Pune	Western Maharashtra plain zone (MH-5)	Drought
Zone-VI			
Gujarat (NGO)	Kutch	North West Zone (GJ-5)	Scanty Rainfall
Gujarat (SAU)	Rajkot	South Saurashtra (GJ-6)	Erratic Monsoon
Gujarat (NGO)	Valsad	South Gujarat Heavy Rainfall (GJ-1)	Heavy Rainfall
Gujarat (ICAR)	Anand	South Gujarat	Drought
Gujarat (ICAR)	Kheda	South Gujarat	Drought
Rajasthan (SAU)	Bharathpur	Flood prone Eastern Plain Zone (RJ-6)	Recurring Flood/ Water Logging
Rajasthan (SAU)	Jhunjhunu	Transitional Plain of Inland Drainage Zone (RJ-3)	Drought/ Erratic Rainfall
Rajasthan (ICAR)	Jodhpur	Arid Western Plain Zone (RJ-1)	Drought/ Heat Wave/ Wind Erosion
Rajasthan (SAU)	Udaipur	Northern Plain and Central Highlands	Drought
Zone-VII			
Chhattisgarh (SAU)	Bilaspur	Chhattisgarh Plain (MP-1)	Drought
Chhattisgarh (SAU)	Dantewada	Bastar Plateau Zone	Soil Erosion/ Heavy Rainfall
Chhattisgarh (SAU)	Raipur	Chhattisgarh Plain (MP-1)	Drought
Chhattisgarh (SAU)	Mahasamund	Eastern Plateau	Drought
Madhya Pradesh (SAU)	Balaghat	Chhattisgarh Plain Zone (MP-1)	Drought
Madhya Pradesh (SAU)	Chhatarpur	Central Narmada Valley Zone (MP-6)	Drought
Madhya Pradesh (SAU)	Guna	Girid Zone (MP-7)	Drought

State	District	Agro-ecological Region	Climatic Hazard
Madhya Pradesh (NGO)	Satna	Kymore, Plateau & Satpura Hill Zone (MP-4)	Drought
Odisha (SAU)	Ganjam	North Eastern Ghat Zone (OR-5)	Drought
Odisha (SAU)	Jharsuguda	Western Central Table Land Zone (OR-9)	Drought/Flood
Odisha (SAU)	Kendrapra	East and South Eastern Coastal Plain Zone (OR-4)	Flood/Cyclone
Odisha (SAU)	Sonepur	Western Central Table Land zone (OR-9)	Drought/Flood
Odisha (SAU)	Ganjam	North Eastern Ghat Zone (OR-5)	Drought
Zone-VIII			
Karnataka (NGO)	Belgaum	Northern Transition Zone (KA-8)	Drought/heat Wave
Karnataka (NGO)	Davangere	Southern Transition Zone (KA-7)	Drought
Karanataka (SAU)	Chickaballapur	Eastern Dry Zone (KA-5)	Drought
Karnataka (ICAR)	Tumkur	Central Dry Zone (KA-4)	Drought
Kerala (ICAR)	Alleppy	Problem areas zone (KE-5)	Salinity/Water Logging
Kerala (SAU)	Palakkad	Western Ghats and Coastal Plains	High temperature
Kerala (SAU)	Thrissur	Western Ghats and Coastal Plains	Drought
Tamil Nadu (SAU)	Namarkkal	North Western Zone (TN-2)	Drought
Tamil Nadu (SAU)	Ramanathapuram	Southern Zone (TN-5)	Drought/ Salinity
Tamil Nadu (SAU)	Villupuram	North Eastern Zone (TN-1)	Drought